World Applied Sciences Journal 16 (9): 1274-1281, 2012
ISSN 1818-4952
© IDOSI Publications, 2012

# Effect of Using Different Troposphere Models on the Resulted Cartesian Coordinates of Processing GPS Short Baselines

*Khaled M. Abdel Mageed*

Department of Civil Engineering, Higher Technological Institute, 10th of Ramadan City, Egypt

**Abstract:** The atmospheric effects can be classified according to the dependency of the signal frequency to two effects. The first effect which depends on the frequency of the signal is called ionospheric effect; while the second effect called tropospheric effect, which is independent on the signal frequency. The tropospheric refraction may be divided into dry and wet components. The dry term contains approximately 90% of the total tropospheric effect and can be predicted to a high degree of accuracy, using mathematical models such as Hopfield, Simplified Hopfield and Saastamoinen models. This paper investigates the effect of using different troposphere models, or in case of not using any troposphere model, on the accuracy of the resulted cartesian coordinates of processing GPS short baselines up to 20km. The results supported by statistical analysis showed that the X coordinate discrepancy between using troposphere model or not using any troposphere model, has mean value of -4.6mm in case of using Hopfield model; -9.2mm in case of using Simplified Hopfield; and -7.2mm in case of using Saastamoinen model. The Y coordinate discrepancy has mean values of -19.1mm, -20.4mm and -18.4mm for the three models as stated before respectively. The Z coordinates have mean values of -12.2mm, -11.9mm and -10.7mm for the three models as stated respectively. Finally, the positional discrepancy has mean value of 23.1mm, 25.3mm and 22.5mm for the three models respectively. These findings are considered to be insignificant in the daily work of cadastral survey; but they should be taken into consideration in case of monitoring the deformation of structures or ancient antiquities, where millimeter accuracy is required.

**Key words:** GPS · Troposphere delay · Hopfield model · Simplified-Hopfield model · Saastamoinen model · No-Troposphere

## INTRODUCTION

The earth's body in the space is covered by the atmosphere, which is composed of different atmospheric layers. At the uppermost part of the earth's atmosphere, ultraviolet and X-ray radiations coming from the sun, interact with the gas molecules and atoms. These interactions result in the so-called gas ionization, which can be defined as: a large number of free negatively charged denoted as electrons and positively charged denoted as atoms and molecules [1]. The basic problem of microwave signals, transmitted by GPS satellites, is that it does not travel along a geometrical straight line, as it would be if it was in vacuum. The code pseudoranges use the so-called group-velocity to determine the traveled signal time, where the phase measurements use the so-called phase-velocity to determine the traveled signal time. Basically, the group velocity is less than phase velocity, thus, the code pseudo-range are measured too long and the carrier phase pseudo-range are measured too short, by the same amount, compared to the geometric distance between the satellite and the receiver [2]. The atmospheric effects can be classified, according to the dependency of the signal frequency, to two effects. The first effect, which depends on the frequency of the signal, is called ionospheric effect [3]. The second effect called tropospheric effect, which is independent on the signal frequency. The tropospheric delay is a function of elevation and altitude of the receiver and is dependent on many factors such as atmospheric pressure, temperature and relative humidity. Unlike the ionospheric delay, the tropospheric delay is not frequency-dependent. It cannot therefore be eliminated through linear combinations of L1 and L2 observations. Several standard tropospheric models such as Hopfield, Simplified Hopfield and Saastamoinen model are generally used to correct for the tropospheric delay [4].

**Corresponding Author:** Khaled M. Abdel Mageed, Department of Civil Engineering, Higher Technological Institute, 10th of Ramadan City, Egypt. E-mail: khaled_mgd@yahoo.com.

All standard tropospheric models are empirically derived from available metrological data, which were mostly obtained in the European and North American continents. Global constants within some standard models take no account of latitudinal and seasonal variations of parameters in the atmosphere [5]. Furthermore, daily variations of temperature and humidity may cause the tropospheric effects derived from standard models to be in error especially in the height component. The high and variable water vapor content, particularly in equatorial regions, may exaggerate this effect further [6]. This paper investigates the effect of using different troposphere models located in common commercial GPS processing software, or not using any troposphere software, on the resulted cartesian X, Y and Z, coordinates and the spatial positional accuracy P; for GPS short baselines up to 20km. The structure of the paper is to introduce the atmosphere effect on the GPS measurements, including the ionosphere and troposphere effect. The most common available troposphere models which are: Hopfield, Simplifies Hopfield and Saastamoinen models are presented with the basic theory and equations. The methodology of investigation and the description of the field test will be presented. Finally, the analysis of the obtained data supported with the statistical analysis will be shown, from which the important conclusions and recommendations will be extracted.

**Troposphere Effect:** The neutral atmosphere can be classified into four layers, namely from bottom to top: troposphere, stratosphere, mesosphere and thermosphere. The troposphere thickness, where temperature decreases with the increase in altitude, is not constant overall the earth's surface. It extends to a height of less than 9 km over the north and south poles and to a height greater than 16 km over the equator [7]. The troposphere has an average thickness of 10 km, in which the temperature remains constant and the stratosphere thickness ranges between 10 and 50 km, where the temperature decreases with height. About 80% of the mass of the above-mentioned layers of the neutral atmosphere lies within the troposphere [8]. The troposphere is a non-dispersive medium for radio frequencies below 15 GHz [9]. Thus, the propagation is frequency independent. As a result, the tropospheric effect delays the GPS carriers and codes identically. Accordingly, the measured satellite to receiver range will be longer than the actual geometric range, which means that, the distance between any two receivers will be longer than the actual distance. On the other hand, the disadvantage of the independency phenomena is that an elimination of tropospheric refraction by dual frequency method is not possible [10]. The tropospheric delay depends on the temperature and the humidity along the signal path through the troposphere region. Signals from satellites at low elevation angles, travel a longer path through the troposphere than those at higher elevation angles. Consequently, the tropospheric delay is minimized at user's zenith and maximized at horizon. For instance, tropospheric delay is about 2.3 m at zenith or when the satellite is overhead the observer and the tropospheric delay is about 9.3 m for 15° elevation angle and about 20 to 25 m at 5° elevation angle [11].

The tropospheric refraction may be divided into dry and wet components. The dry term contains approximately 90% of the total tropospheric effect and can be predicted to a high degree of accuracy, using mathematical models. It can accurately be modeled up to 95% from surface meteorological data, such as pressure, humidity and temperature [7]. On the other hand, the wet component is not easy to predict, where it depends on the water vapor along the signal path. There are various models available to date such as Hopfield and Saastamoinen to model for this component taking into account such factors as the water vapor content, temperature, altitude and the elevation angle of the signal path [12]. However the wet component is weakly correlated with surface metrological data, which is limiting the prediction accuracy, it was found that using default metrological data, which are 20°C, 1010 mb pressure and 50% relative humidity, gave satisfactory results in most cases [13]. Practically, tropospheric effect almost completely cancelled out using differencing modes of observations, if the stations are close together. Accordingly, it is not advisable to introduce the observed meteorological data separately for each station into the adjustment of a small network in non-mountainous regions. The local measurements usually do not rigorously represent the regional atmospheric situation and hence introduce biases into the solution. Instead, appropriate identical standard atmospheric parameters should be used for all stations of the considered network [14]. On the other hand, when station distance increases, or when height difference between baselines ends increases, such as in mountainous areas, the local atmospheric conditions are no longer sufficiently correlated with each other. In such a case, the residual atmospheric delay will be large enough to be taken into account in the adopted observation equation. However, adequate modeling of this residual tropospheric delay is something difficult, particularly for the wet delay component [13].

**Review of Some Tropospheric Models:** In this section, a simple presentation of the mathematical model of some tropospheric models will be presented. These models are Hopfield, Simplified Hopfield and Saastamoinen models. The tropospheric path delay is defined by Hofmann *et al.* [13]:

$$\Delta^{trop} = 10^{-6}\int N^{trop}.\ dS \quad (1)$$

Where:

$\Delta^{trop}$ is the tropospheric delay
$N^{trop}$ is the refractivity

The tropospheric delay can be separated into dry and wet components as follow:

$$\Delta_d^{trop} = 10^{-6}\int N_d^{trop}\ dS \quad (2)$$

$$\Delta_w^{trop} = 10^{-6}\int N_w^{trop}\ dS \quad (3)$$

$$\Delta^{trop} = \Delta_d^{trop} + \Delta_w^{trop} \quad (4)$$

$$\Delta^{trop} = 10^{-6}\int N_d^{trop}\ dS + 10^{-6}\int N_d^{trop}\ dS \quad (5)$$

Practically the integration is performed by numerical methods or series expansions. The dry component at the surface can be calculated from:

$$N_{d,0}^{trop} = 77.64\frac{P}{T} \quad (6)$$

Where P is the atmospheric pressure in millibar and T is the temperature in Kelvin.
In addition, the wet component can be expressed as:

$$N_{w,0}^{trop} = 12.96\frac{e}{T} + 3.718x10^5\frac{e}{T^2} \quad (7)$$

Where: e is the partial pressure of water vapor in millibar.

**Hopfield Model:** Using real data covering the whole earth, Hopfield has empirically found a representation of the dray refractivity as a function of height h above the surface by Hopfield [15]:

$$N_d^{trop}(h) = N_{d,0}^{trop}\left[\frac{h_d - h}{h_d}\right]^4 \quad (8)$$

Where $h_d$ is the height of the dry troposphere layer and can be calculated from:

$$h_d = 40136 + 148.72\,(T - 273.16) \quad (9)$$

Substitution of equations 6 and 7 into 2 and make an integration of the vertical direction with an observation site on the surface of the earth (i.e. h=0), yields to the dry portion of the tropospheric zenith delay:

$$\Delta_d^{trop} = \frac{10^{-6}}{5}N_{w,0}^{trop}\ h_d \quad (10)$$

Hopfield model assumes the same functional model for both wet and dry components although the wet portion is much difficult to model because of the strong variations of the water vapor.

Analogously:

$$N_w^{trop}(h) = N_{w,0}^{trop}\left[\frac{h_w - h}{h_w}\right]^4 \quad (11)$$

Where the mean value of $h_w$=11000m.

The integration of the above equation is completely analogous to equation 8, therefore:

$$\Delta_w^{trop} = \frac{10^{-6}}{5}N_{w,0}^{trop}\ h_w \quad (12)$$

Accordingly, the total tropospheric zenith delay is:

$$\Delta^{trop} = \frac{10^{-6}}{5}\left[N_{d,0}^{trop}.h_d + N_{w,0}^{trop}.h_w\right] \quad (13)$$

The above equation dos not account for an arbitrary zenith angle, to overcome this problem, the transition of the zenith delay to a delay with arbitrary zenith angle is performing by the application of a mapping function. After adding the mapping function effect, eq. 10 will be:

$$\Delta^{trop} = \frac{10^{-6}}{5}\left[N_{d,0}^{trop}.h_d.m_d(E) + N_{w,0}^{trop}.h_w m_w(E)\right] \quad (14)$$

The mapping functions for the dry and wet components are defined as:

$$m_d(E) = \frac{1}{sin\sqrt{E^2 + 6.25}} \text{ and } m_w(E) = \frac{1}{sin\sqrt{E^2 + 2.25}} \quad (15)$$

Where: E is the elevation at the observing site (in degrees).

**Simplified Hopfield Model:** A modification to Hopfield model is introduced by replacing lengths of the position vectors instead of heights in equation 8. The dry refractivity will be:

$$N_d^{trop}(r) = N_{d,0}^{trop}\left[\frac{r_d - r}{r_d - R_E}\right]^4 \quad (16)$$

Where:

$R_E$ : The radius of the earth
$r_d$ : The radius of the dry layer; $r_d = R_E + h_d$
r : The radius of any observation site at h above the surface of the earth; $r = R_E + h$

Applying the mapping functions, the final dry model will be:

$$\Delta_d^{trop}(z) = \frac{10^{-6}N_{d,0}^{trop}}{(r_d - R_E)^4}\int_{r=R_E}^{r=r_d}\frac{r(r_d - r)^4}{\sqrt{r^2 - R_E^2 sin^2 z_0}}dr \quad (17)$$

Analogously, the wet component can be written as:

$$\Delta_w^{trop}(z) = \frac{10^{-6}N_{w,0}^{trop}}{(r_w - R_E)^4}\int_{r=R_E}^{r=r_w}\frac{r(r_w - r)^4}{\sqrt{r^2 - R_E^2 sin^2 z_0}}dr \quad (18)$$

Several models are derived depending on the method of solving the integral, the most common one is:

$$\Delta_d^{trop}(E) = 10^{-12}N_{d,0}^{trop}\left[\sum_{k=1}^{9}\frac{\alpha_k}{k}r_d^k\right] \quad (19)$$

Where: E is the elevation angle for the zenith angle z

$$E = 90° - z$$
$$r_d = \sqrt{(R_E + h_d)^2 - (R_E \cos E)^2} - R_E sin\, E \quad (20)$$

The parameters $\alpha_1$ to $\alpha_9$ are defined as follow:

$$A = \frac{Sin\ E}{h_d} \qquad B = \frac{Cos^2 E}{2 h_d R_E}$$

$$\alpha_1 = 1 \quad \alpha_2 = 4A \quad \alpha_3 = 6A^2 + 4B$$
$$\alpha_4 = 4A(A^2 + 3B) \quad \alpha_5 = A^4 + 12AB + 6B^2 \quad \alpha_6 = 4AB(A^2 + 3B)$$
$$\alpha_7 = B^2(6A^2 + 4B) \quad \alpha_8 = 4AB^3 \quad \alpha_9 = B^4 \quad (21)$$

Analogously, the same set of the above equations will be valid for the wet part, after replacing any dry component with the symmetric wet component.

**Saastamoinen Model:** In this model, the refractivity can be determined from the gas low. The model can be written as Saastamoinen [16]:

$$\Delta^{tropo} = \frac{0.002277}{cosz}\left[p + \left(\frac{1255}{T} + 0.05\right)e - tan^2 z\right] \quad (22)$$

Where z is the zenith angle of the satellite, T is the temperature at the station in units of Kelvin, P is the atmospheric pressure in units of mbar and e is the partial pressure of water vapor in mbar.

$$e = R_h \exp(-37.2465 + 0.213166T - 0.000256908T^2) \quad (23)$$

Where $R_h$ is the relative humidity in % and exp () is the exponential function. To transform the unit of the temperature T from Kelvin K to Celsius, one may use:

$$T\ (Kelvin) = T\ (Celsius) + 273.16 \quad (24)$$

In this model, either measured values of pressure, temperature and humidity are used; or values derived from standard atmospheric model can be used by the equations:

$$P = P_0\,[1 - 0.000226\,(H - H_0]^{5.225} \quad (25)$$

$$T = T_0 - 0.0065\,(H - H_0) \quad (26)$$

$$R_h = R_{h0} \exp\,[-0.0006396\,(H - H_0)] \quad (27)$$

Where $P_0$ = 1013.25 mbar, $T_0$ = 18° Celsius and $R_{h0}$ = 50% are called standard pressure, temperature and humidity at the reference height $H_0$ = 0 m [17].

**Methodology of Investigation:** The objective of this paper is to statically analyze the difference in 3-d coordinates resulted from processing GPS baselines up to 20 km, using different troposphere models, or in case of not using any troposphere models. The methodology of this paper will be based on comparing the 3-d Cartesian coordinates of 8 GPS baselines with approximate distances from 2.5 km to 20 km, which were processed using Hopfield, Simplified Hopfield, Saastamoinen and No troposphere models. The field test was conducted at New Cairo City on Aug 2, 2011 and Aug 4, 2011. A dual frequency GPS receiver of Topcon GR3 was setup at a reference control point. A second dual frequency receiver of the same type of Topcon GR3 was set up sequentially on 8 control points of approximate distances from 2.5 km to 20 km, from the base station. The observational operating parameters were the same for the two receivers, which are: static mode, elevation angle 15° and 10 seconds rate of observations. The observational duration of each baseline was as follows: 25 minutes for the baselines of approximate distance 2.5 km and 5 km; 45 minutes for the baselines of approximate distances 7.5 km, 10 km and 12.5 km; 65 minutes for the baselines of approximate distances 15 km, 17.5 km and 20 km. The raw data of the GPS campaign were downloaded and transferred to Rinex format using Topcon Link software. The processing of the Rinex data was conducted using Leica Geo Office software. The data were processed using Hopfield, Simplified Hopfield, Saastamoinen and No troposphere models. The 3-d cartesian coordinates for every troposphere model were archived for the statistical analysis.

**Analysis of Results:** The analysis of the results will be based on comparing the discrepancies in X, Y and Z coordinates between processing 8 GPS baselines using Hopfield, Simplified Hopfield and Saastamoinen, against processing the same baselines without any troposphere model.

$$\begin{aligned} \Delta X_{No-Hop} &= X_{No} - X_{Hop} \\ \Delta Y_{No-Hop} &= Y_{No} - Y_{Hop} \\ \Delta Z_{No-Hop} &= Z_{No} - Z_{Hop} \end{aligned} \qquad (28)$$

Where: $\Delta X_{No\text{-}Hop}$, $\Delta Y_{No\text{-}Hop}$ and $\Delta Z_{No\text{-}Hop}$: the X, Y and Z discrepancies between using Hopfield model and without using any troposphere model.

$X_{No}$, $Y_{No}$ and $Z_{No}$: the X, Y and Z coordinates resulted from using No model troposphere.

$X_{Hop}$, $Y_{Hop}$ and $Z_{Hop}$: the X, Y and Z coordinates resulted from using Hopfield troposphere model.

The same set of equations no. 28 can be rewritten for both Simplified Hopfield and Saastamoinen troposphere models as follows:

$$\begin{aligned} \Delta X_{No-S.Hop} &= X_{No} - X_{S.Hop} \\ \Delta Y_{No-S.Hop} &= Y_{No} - Y_{S.Hop} \\ \Delta Z_{No-S.Hop} &= Z_{No} - Z_{S.Hop} \end{aligned} \qquad (29)$$

Where: $X_{S.Hop}$, $Y_{S.Hop}$ and $Z_{S.Hop}$: the X, Y and Z coordinates resulted from using Simplified Hopfield troposphere model.

$$\begin{aligned} \Delta X_{No-Sast} &= X_{no} - X_{Sast} \\ \Delta Y_{No-Sast} &= Y_{no} - Y_{Sast} \\ \Delta Z_{No-Sast} &= Z_{no} - Z_{Sast} \end{aligned} \qquad (30)$$

Where: $X_{S.Hop}$, $Y_{S.Hop}$ and $Z_{S.Hop}$: the X, Y and Z coordinates resulted from using Simplified Hopfield troposphere model. On the other hand, the positional discrepancies ΔP and Standard Deviation $\sigma_{\Delta p}$ for every pairs of solutions can be written as:

$$\begin{aligned} \Delta P_{No-Hop} &= \sqrt{\Delta X^2_{No-Hop} + \Delta Y^2_{No-Hop} + \Delta Z^2_{No-Hop}} \\ \Delta P_{No-S.Hop} &= \sqrt{\Delta X^2_{No-S.Hop} + \Delta Y^2_{No-S.Hop} + \Delta Z^2_{No-S.Hop}} \\ \Delta P_{No-Sast} &= \sqrt{\Delta X^2_{No-Sast} + \Delta Y^2_{No-Sast} + \Delta Z^2_{No-Sast}} \end{aligned} \qquad (31)$$

$$\begin{aligned} \sigma^2_{\Delta PNo-Hop} &= \sigma^2_{\Delta X\,No-Hop} + \sigma^2_{\Delta Y\,No-Hop} + \sigma^2_{\Delta Z\,No-Hop} \\ \sigma^2_{\Delta PNo-S.Hop} &= \sigma^2_{\Delta X\,No-S.Hop} + \sigma^2_{\Delta Y\,No-S.Hop} + \sigma^2_{\Delta Z\,No-S.Hop} \\ \sigma^2_{\Delta PNo-Sast} &= \sigma^2_{\Delta X\,No-Sast} + \sigma^2_{\Delta Y\,No-Sast} + \sigma^2_{\Delta Z\,No-Sast} \end{aligned} \qquad (32)$$

The discrepancies in X, Y, Z and position P, between processing the GPS data using Hopfield and using No-Trop are shown in Table 1.

The Cartesian coordinates X, Y and Z between using Hopfield and No-Trop models are illustrated in Fig. 1.

Table 1 and Fig. 1 are supported by descriptive statistics to measure the quality of the obtained results. Table 2 shows these descriptive statistics. For instance, the X-coordinate discrepancies are ranging between 9.8 mm and -27.3mm, with mean value -4.6mm and SD 13.4mm for single determination. The Y-coordinate discrepancies are fluctuating between 11.6mm and -61.1mm, with mean value of -19.1mm and SD for single observation of 28.1mm. The Z-coordinate discrepancies are varying between 4.8mm and -42.7mm, with mean value of -12.2mm and SD for single determination of 16.2 mm. Finally, the positional discrepancies P between using Hopfield and No-Trop models are differing from 8.4mm to 79.4mm, with most probable value of 23.1mm and SD 26.4mm, respectively. The previous set of tables and figure were created again between processing the GPS data using Simplified–Hopfield model and using No-Trop model. Accordingly, the findings are tabulated in Tables 3 and 4 and Fig. 2.

For example, the positional discrepancy P between Simplified-Hopfield and No-Trop models are ranging between 8.4 mm and 88.2 m with mean value of 25.3 mm and standard deviation of 29.9 mm for single determination. The last set of tables and figures is the comparison of results between processing the GPS data using Saastamoinen model and using No-Trop model. In this regard, the results are tabulated in Tables 5 and 6 and Fig. 3.

Table 1: The discrepancies in X, Y, Z and position P between Hopfield and No-Trop models

| Baseline No. | Approx. Length (km) | Δ X (mm) | Δ Y (mm) | Δ Z (mm) | Δ P (mm) |
|---|---|---|---|---|---|
| 1 | 2.5 | 9.8 | 5.7 | 2.1 | 11.5 |
| 2 | 5.0 | 3.0 | 6.6 | -4.2 | 8.4 |
| 3 | 7.5 | 9.4 | -3.9 | -6.6 | 12.1 |
| 4 | 10.0 | 3.7 | 11.6 | -6.5 | 13.8 |
| 5 | 12.5 | -8.4 | -23.9 | 4.8 | 25.8 |
| 6 | 15.0 | -9.5 | -38.3 | -16.1 | 42.6 |
| 7 | 17.5 | -17.7 | -49.3 | -28.7 | 59.7 |
| 8 | 20.0 | -27.3 | -61.1 | -42.7 | 79.4 |

Table 2: Descriptive statistics of the discrepancies between Hopfield and No-Trop models (mm)

| Descriptive | Max. | Min. | Range | Mean | $S.D_{single}$ | $S.D_{mean}$ |
|---|---|---|---|---|---|---|
| ΔX | 9.8 | -27.3 | 37.1 | -4.6 | 13.4 | 4.7 |
| ΔY | 11.6 | -61.1 | 72.7 | -19.1 | 28.1 | 9.9 |
| ΔZ | 4.8 | -42.7 | 47.5 | -12.2 | 16.2 | 5.7 |
| ΔP | 79.4 | 47.5 | 71.0 | 23.1 | 26.4 | 9.3 |

Table 3: The discrepancies in X, Y, Z and position P between Simplified-Hopfield and No-Trop models

| Baseline No. | Approx. Length (km) | Δ X (mm) | Δ Y (mm) | Δ Z (mm) | Δ P (mm) |
|---|---|---|---|---|---|
| 1 | 2.5 | 10.4 | 6.4 | 2.5 | 12.5 |
| 2 | 5.0 | 3.1 | 6.7 | -4.0 | 8.4 |
| 3 | 7.5 | -9.5 | 3.6 | 6.0 | 11.8 |
| 4 | 10.0 | 4.4 | 12.3 | -5.8 | 14.3 |
| 5 | 12.5 | -11.4 | -26.8 | 2.1 | 29.2 |
| 6 | 15.0 | -13.8 | -42.5 | -18.8 | 48.5 |
| 7 | 17.5 | -23.2 | -55.3 | -30.7 | 67.4 |
| 8 | 20.0 | -33.3 | -67.3 | -46.3 | 88.2 |

Table 4: Descriptive statistics of the discrepancies between Simplified-Hopfield and No-Trop models (mm)

| Descriptive | Max. | Min. | Range | Mean | $S.D_{single}$ | $S.D_{mean}$ |
|---|---|---|---|---|---|---|
| ΔX | 10.4 | -33.3 | 43.7 | -9.2 | 14.8 | 5.2 |
| ΔY | 12.3 | -67.3 | 79.6 | -20.4 | 31.7 | 11.2 |
| ΔZ | 6.0 | -46.3 | 52.3 | -11.9 | 18.5 | 6.6 |
| ΔP | 88.2 | 8.4 | 79.8 | 25.3 | 29.9 | 10.6 |

Table 5: The discrepancies in X, Y, Z and position P between Saastamoinen and No-Trop models

| Baseline No. | Approx. Length (km) | Δ X (mm) | Δ Y (mm) | Δ Z (mm) | Δ P (mm) |
|---|---|---|---|---|---|
| 1 | 2.5 | 9.8 | 5.7 | 2.1 | 11.5 |
| 2 | 5.0 | 3.0 | 6.6 | -4.1 | 8.3 |
| 3 | 7.5 | -9.4 | 3.8 | 6.5 | 12.0 |
| 4 | 10.0 | 3.7 | 11.6 | -6.4 | 13.8 |
| 5 | 12.5 | -8.5 | -23.9 | 4.7 | 25.8 |
| 6 | 15.0 | -9.6 | -38.3 | -16.2 | 42.7 |
| 7 | 17.5 | -19.0 | -51.1 | -29.7 | 62.1 |
| 8 | 20.0 | -27.8 | -61.6 | -42.7 | 79.9 |

Table 6: Descriptive statistics of the discrepancies between Saastamoinen and No-Trop models (mm)

| Descriptive | Max. | Min. | Range | Mean | $S.D_{single}$ | $S.D_{mean}$ |
|---|---|---|---|---|---|---|
| ΔX | 9.8 | -27.8 | 37.6 | -7.2 | 12.5 | 4.4 |
| ΔY | 11.6 | -61.6 | 73.2 | -18.4 | 29.2 | 10.3 |
| ΔZ | 6.5 | -42.7 | 49.2 | -10.7 | 17.6 | 6.2 |
| ΔP | 79.9 | 8.3 | 71.6 | 22.5 | 26.9 | 9.5 |

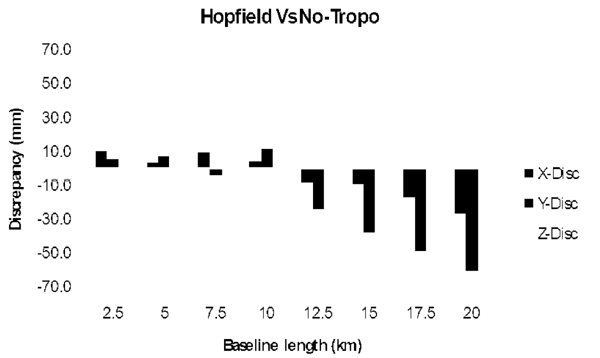


Fig. 1: Variation of the X, Y and Z coordinate discrepancies between Hopfield and No-Trop models

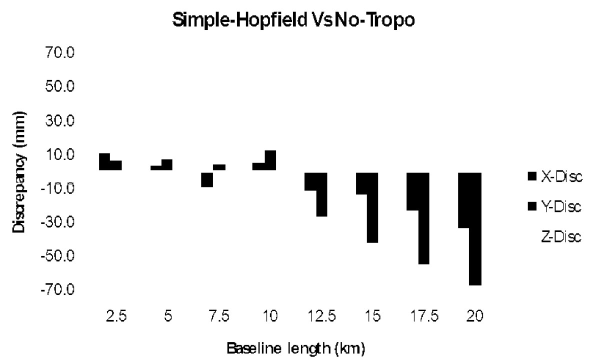


Fig. 2: Variation of the X, Y and Z coordinate discrepancies between Simplified-Hopfield and No-Trop models

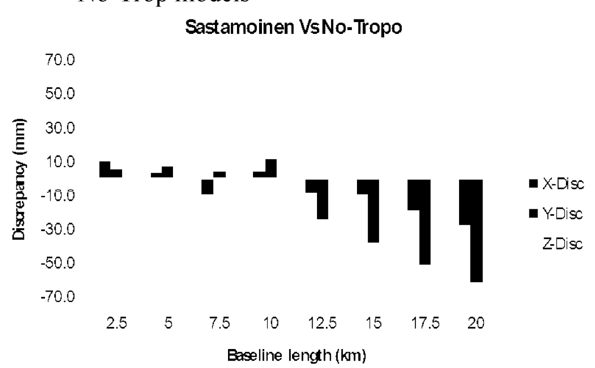


Fig. 3: Variation of the X, Y and Z coordinate discrepancies between Saastamoinen and No-Trop models

For example, the positional discrepancy P between Saastamoinen and No-Trop models are ranging between 8.3 mm and 79.9 mm with mean value of 22.5 mm and standard deviation of 26.9 mm for single determination. The positional discrepancies between each Troposphere model (Hopfield, Simplified Hopfield and Saastamoinen) and No-Trop model are displayed in Fig. 4.

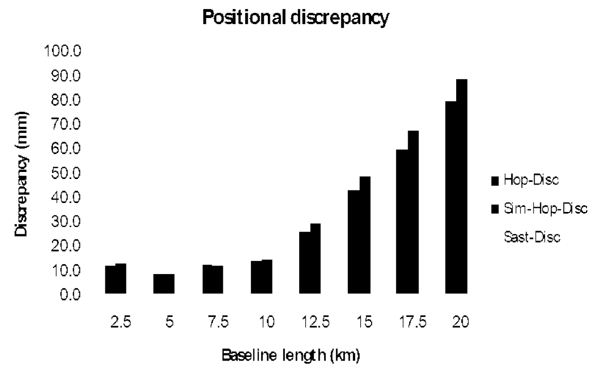


Fig. 4: Positional discrepancies between each Tropo model and No-Trop model

## CONCLUSIONS

The present study discusses the effect of using different troposphere models on the resulted Cartesian coordinates resulted from processing GPS short baselines up to 20km. A GPS campaign was conducted to observe 8 baselines varying from 2.5km to 20km. The GPS data were processed using three different troposphere models namely: Hopfield, Simplified-Hopfield and Saastamoinen models. The Cartesian coordinates resulted from using each troposphere model was compared with the resulted cartesian coordinates from using No-Troposphere model.

The statistical analysis of the obtained results showed the following:

- The discrepancies in X, Y and Z coordinates between using Hopfield model and using No-Troposphere model have mean values of -4.6 mm, -19.1 mm and -12-2 mm respectively. The standard deviations for single determination for the previous findings are 13.4 mm, 28.1 mm and 16.2 mm respectively.
- The discrepancies in X, Y and Z coordinates between using Simplified-Hopfield and No-Troposphere models have mean values of -9.2 mm, -20.4 mm and -11.9 mm. The standard deviations for the previous values are 14.8 mm, 31.7 mm and 18.5 mm respectively.
- The discrepancies in X, Y and Z coordinates between using Saastamoinen and No-Troposphere models have mean values of -7.2 mm, -18.4 mm and -10.7 mm. The standard deviations for the previous values are 12.5 mm, 29.2 mm and 17.6 mm respectively.

- The positional discrepancies between each one of the troposphere models compared to using No-Troposphere model have mean values of 23.1 mm with SD 26.4 mm for Hopfield model; 25.3 mm with SD 29.9 mm for Simplified-Hopfield model and 22.5 mm with SD 26.9 mm for Saastamoinen model.

The above results are considered to be insignificant in the daily work of cadastral survey; but it should be taken into consideration in case of monitoring the deformation of structures or ancient antiquities, where millimeter accuracy is required. In this respect, it is recommended to process the GPS data using the same troposphere model to maintain the accuracy of millimeter.

## REFERENCES

1. Seeber, G., 1993. Satellite Geodesy: Foundations, Methods and Applications. Walter De Gruyter, Berlin.
2. Rizos, C., 1997. Principles and Practice of GPS Surveying. Monograph 17, School of Geomatics Engineering, the University of New south Wales.
3. Klobuchar, J.A., 1991. Ionospheric Effects on GPS. GPS World, 2(4): 48-51.
4. Langley, R.B., 1992. The effect of the ionosphere and troposphere on satellite positioning system. The Symposium on Refraction of Transatmospheric Signals in Geodesy. Netherlands.
5. Roberts, C. and C. Rizos, 2001. Mitigating differential troposphere for GPS-based volcano monitoring. Proceeding of the 5th International Symposium on Satellite Navigation Technology and applications, Canberra, Australia.
6. Grant, D.B., C. Rizos and A. Stolz, 1990. Dealing with GPS Biases; some Theoretical and Software Considerations. School of Surveying, University of New South Wales, Australia.
7. Leick, A., 1995. GPS Satellite Surveying. A Willey Inter-Science Publications, John Willey and Sons, New York.
8. Kaplan, E., 1996. Understanding GPS: Principles and Applications. Norwood, MA: Artech House.
9. Chao, C.C., 1972. A model for tropospheric calibration from daily surface and radiosonde balloon measurements. JPL technical memorandum, Jet Propulsion Laboratory, Pasadena, CA.
10. Brunner, F. K. and W.M. Welsch, 1993. Effect of the troposphere on GPS measurements. GPS World, 4(1): 42-51.
11. Shaw, M., K. Sandhoo and D. Turner, 2000. Modernization of the Global Positioning System. GPS World, 11(9): 36-44.
12. Hay, C. and J. Wong, 2000. Enhancing GPS: tropospheric delay prediction at the master control station. GPS World, 11(1): 56-62.
13. Hofmann-Wellenhof, B., H. Lichtenegger and J. Collins, 2001. Global Positioning System - Theory and Practice. 5th Revised Edition, Springer-Verlag, New York.
14. Seeber, G., 2003: Satellite Geodesy. 2nd Ed., Walter de Gruyter, Berlin, pp: 589.
15. Hopfield, H.S., 1971. Tropospheric effect on electromagnetically measured range: predicted from surface weather data. Radio Sci., 6(3): 357-367.
16. Saastamoinen, J., 1973. Contributions to the theory of atmospheric refraction. Bulletin of Géodésique, 107: 13-34.
17. Guochang, Xu, 2007. GPS Theory, Algorithms and Applications. 2nd Edition, Springer Publishing, New York.